

UNCLASSIFIED

AD NUMBER
ADB952994
NEW LIMITATION CHANGE
TO Approved for public release, distribution unlimited
FROM Distribution authorized to U.S. Gov't. agencies and their contractors; Foreign Government Information; OCT 1953. Other requests shall be referred to British Embassy, 3100 Massachusetts Ave., NW, Washington, DC 20008.
AUTHORITY
DSTL ltr, 28 Sep 2009

THIS PAGE IS UNCLASSIFIED

C.P. No. 220  
(16,576)  
A.R.C. Technical Report

FILE  
R

BR 78931  
C.P. No. 220  
(16,576)  
A.R.C. Technical Report

UNANNOUNCED

BRITISH  
LIBRARY



1

AD B 952994

MINISTRY OF SUPPLY

AERONAUTICAL RESEARCH COUNCIL

9 CURRENT PAPERS

DTIC  
ELECTE  
JUN 22 1981

6

On the Laminar  
Boundary Layer Separation  
from the Leading edge of a  
Thin Aerofoil.

By

10 P. R. Owen ~~and~~ L. Klanfer B.Sc.

Best Available Copy

16 Oct 53

18 DRIC, RAE

12 21

19 BR 78931  
AERO 2508

14 ARC-CP-220,  
ARC-TR-16576

LONDON: HER MAJESTY'S STATIONERY OFFICE

1955

DTIC FILE COPY

008450

RT 6 10 010

ADDENDUM

After this paper had been discussed by the Fluid Motion sub-committee of the Aeronautical Research Council, Dr. G. K. Batchelor kindly sent the authors a copy of a paper written by him in 1943 ('The Laminar Flow Characteristics of Three Related Aerofoils', Australian C.S.I.R. Report A.20) in which he described observations of the laminar boundary layer separation from an aerofoil and its subsequent reattachment as a turbulent layer. He, too, conjectured that  $l/\delta^*$  or  $U_\infty l/\nu$  would be a function of  $(R\delta^*)_s$ , although all his results were confined to what we have called 'short bubbles'.

Batchelor's measurements, which relate to separation from a point towards the rear of the aerofoil at small incidence, are not inconsistent with Figures 2 and 3 of this paper, and are shown in the Table below.

$l/\delta^*$	$(R\delta^*)_s$
40	1060
39	1200
43	1680
54	2380
34	2910
21	3360
6	3760

Accession For	
NTIS GRA&I	<input type="checkbox"/>
DTIC TAB	<input type="checkbox"/>
Unannounced	<input checked="" type="checkbox"/>
Justification	
By _____	
Distribution/_____	
Availability Codes	
Dist	Avail and/or Special
12	

1955  
 CONTROLLER  
 HMSO LONDON

532.526.2/5:533.69.042.8:533.6.011.12

Report No. Aero 2508

October, 1953

ROYAL AIRCRAFT ESTABLISHMENT.

"On the laminar boundary layer separation  
from the leading edge of a thin aerofoil"

by

P. R. Owen, B.Sc.

and

L. Klanfer, B.Sc.

SUMMARY

Low speed wind tunnel tests have shown that when a laminar boundary layer separates from the leading edge of a thin aerofoil at incidence the flow often becomes attached to the surface again some distance downstream. The region of separated flow is called a bubble and its chordwise dimension may vary from a minute fraction of the chord to a length comparable with the chord, depending on incidence, Reynolds number and type of aerofoil section. In this respect, a marked contrast between the lengths of bubble on the N.A.C.A. 63-009 and 64-006 sections was found in tests at Langley Field.

It is suggested that the length of bubble (more accurately, its order of magnitude compared with the thickness of the laminar boundary layer at separation) depends primarily on the Reynolds number  $(R_{\delta^*})_s$  based on the displacement thickness at the separation point; if  $(R_{\delta^*})_s$  exceeds 400-500, the bubble is short: if less than this band of values, the bubble may be long.  $(R_{\delta^*})_s$  in turn depends on the distance of the velocity peak on the upper surface of the aerofoil from the front stagnation point and it is inferred that, at a given Reynolds number based on the chord, a long bubble is more likely to occur when the velocity peak is close to the stagnation point: but a scale effect, such as to cause the bubble to change from long to short as the Reynolds number is increased beyond a critical value, can also be expected.

These observations are used to comment on certain peculiarities in the stalling behaviour of thin sweptback wings.

### LIST OF CONTENTS

	<u>Page</u>
1 Introduction	3
2 Some experimental results	3
2.1 Definitions of long and short bubbles	4
3 The mechanism of flow reattachment	5
4 Analysis of experimental data	6
4.1 Variation in the length of bubble with Reynolds number at separation	7
5 Discussion	9
6 Future developments	11
7 Conclusions	11
References	13

### LIST OF TABLES

	<u>Table</u>
Length of bubble/wing chord	I
Length of bubble/displacement thickness	II
Comparison between the observed and estimated positions of the laminar separation point	III
Relation between type of bubble and boundary layer Reynolds number at separation	IV
$(R \delta^v)_s \left( \frac{U_m x_m}{\nu} \right)^{\frac{1}{2}}$	V
Length of bubble and boundary layer Reynolds number at separation	VI

### LIST OF ILLUSTRATIONS

	<u>Figure</u>
Lift curves for sections of 6% and 9% thickness/chord ratio	1
Variation of length of separated flow region with boundary layer Reynolds number at the separation point	2
Variation of $\frac{U_s \ell}{\nu}$ with boundary layer Reynolds number at the separation point	3
Relation between velocity at separation and maximum velocity	4
Maximum lift of N.A.C.A. cambered aerofoil sections	5

## 1 Introduction

It is well known that at low subsonic speeds, the laminar boundary layer on a thin aerofoil separates from the upper surface at a point very near the leading edge if the incidence is sufficiently high. The cause, obviously enough, is the severe adverse pressure gradient that develops in the neighbourhood of the sharply curved nose. Until recently the phenomenon was not considered to have much practical aeronautical significance, since wings in common use were of such thickness (greater than 0.1 chord) that the stall usually began near the trailing edge in the form of a turbulent boundary layer separation. But wings - for military aircraft at least - have now to be designed for satisfactory operation at high Mach numbers, with the inevitable trend towards small thickness/chord ratios, and laminar separation from the forward parts of the profile has emerged as a serious practical problem.

At large Reynolds numbers, in excess of  $10^6$  based on the chord, and with wings having a finite, but small, nose radius of curvature the separated flow generally becomes attached to the surface again as a turbulent boundary layer, and the region between the points of separation and reattachment is often graphically referred to as a "bubble". The extent of the bubble on two-dimensional wings has been found in experiment to vary from a tiny proportion of the chord - less than  $0.1\%$  - to something comparable with the chord length, and this paper is concerned with the particular problem of explaining the mechanism that controls the length of bubble.

## 2 Some experimental results

The behaviour of the bubble as the incidence is altered has a powerful influence on the stalling characteristics of the wing; in particular, the contrast between a wing with a small bubble and one with an extensive bubble has been demonstrated in some remarkably detailed wind tunnel experiments made by N.A.C.A.<sup>1,2</sup>. Two symmetrical aerofoils were tested, one of N.A.C.A. 64-006 and the other of N.A.C.A. 63-009 section; in both cases the Reynolds number was  $5.8 \times 10^6$ . At small incidences it was found that a minute bubble developed near the leading edges of both wings. The bubble on the thinner wing rapidly enlarged as the incidence exceeded  $5^\circ$  and with further increase of incidence became progressively longer until it extended over the entire chord, at which stage the wing could be regarded as completely stalled. On the other hand, there was little change in the length of bubble on the thicker wing up to a certain incidence; beyond this, the bubble suddenly "burst", causing the aerofoil to stall abruptly. This "bursting" can be interpreted as a failure of the separated flow to reattach itself to the surface. The lengths of bubble on the two wings are compared in the Table below.

TABLE I

Length of bubble/wing chord

Incidence (degrees)	Length of bubble/(wing chord)	
	64-006 section	63-009 section
5	0.08	0.0052
6	0.23	0.0048
7	0.40	0.0034
8	0.56	0.0022
9	Upper surface stalled	Upper surface stalled

The sequence of events described above can be traced in the lift curves which are reproduced in Fig.1. The lift on the 6% thick section, shown in Fig.1 (a), rises linearly with incidence as far as roughly 5° when a rapid change, amounting practically to a discontinuity, occurs. This stage corresponds to the sudden enlargement of the region of separated flow. For incidences greater than 5° the lift rises again, but with a reduced gradient attributable to the progressive spreading of the separation bubble along the upper surface. In the neighbourhood of 9° incidence the downstream end of the bubble reaches the trailing edge, resulting in a gentle stall.\* The lift curve for the 9% thick section is markedly different. It is quite straight up to an incidence of 9°; at the stall, the lift falls catastrophically owing to the violent disruption of the bubble.

### 2.1 Definitions of "long" and "short" bubbles

The bubble on the thinner wing will be seen from Table I to be from 10 to 100 times longer than that on the thicker wing, in terms of the chord. While this description serves to distinguish between long and short bubbles on these particular sections, it is not convenient for a general discussion; for this purpose, it is preferable to relate the size of bubble to some length characteristic of the boundary layer at the point of separation, and we shall here choose the displacement thickness. Writing  $\delta^*_s$  for the displacement thickness at separation, which can be calculated by the methods referred to in Section 4, and  $l$  for the length of bubble, some typical ratios of  $l/\delta^*_s$  for the two N.A.C.A. aerofoils are shown in the Table below.

TABLE II

Length of bubble/displacement thickness

Incidence (degrees)	$l/\delta^*_s$	
	64-006 Section	63-009 Section
6	5,440	77
7	8,800	67
8	12,890	46

The figures in Table II suggest the following definitions:

$$\begin{aligned} \text{short bubble; } l/\delta^*_s &\sim 10^2 \\ \text{long bubble; } l/\delta^*_s &\sim 10^4 \end{aligned}$$

It will be demonstrated later that these definitions have a greater generality than the few values given in Table II might imply.

\* The different regimes of flow can also be related to the behaviour of the centre of pressure. Between zero and 5° the centre of pressure remains fixed a short distance aft of the  $\frac{1}{4}$ -chord point on the aerofoil. As the incidence is increased beyond 5° the centre of pressure at first moves slightly forward then, at about 6°, moves aft; the aft movement is especially rapid as the stall is approached. These variations in centre of pressure position can be explained qualitatively by regarding the bubbles as a region of quiescent flow in which the pressure is nearly constant. Thus, as the bubble grows, the pressure on the wing becomes more uniformly distributed along the chord. Initially, this happens near the leading edge, giving rise to a forward centre of pressure movement; subsequently it extends over a large part of the chord, so redistributing the lift as to cause the centre of pressure to move aft.

### 3 The mechanism of flow reattachment

The contrasting behaviour of the 6% and 9% thick aerofoils described in the previous Section brings out quite plainly the importance of the laminar separation bubble and the way it spreads with change of incidence. The questions which naturally follow this observation are: (a) can we predict from some property of the aerofoil, such as the pressure distribution over its upper surface, whether the bubble will be long or short?; (b) can it be assumed that the type of bubble found at wind tunnel Reynolds numbers will persist at full scale? In many respects the second question is the more important.

Before attempting to answer these questions we must construct some hypothesis concerning the reattachment of the separated flow to the surface of the wing, and the rapidity with which it occurs. For the mechanism of reattachment, there is ample evidence\* to show that transition to turbulence takes place in the bubble and the subsequent turbulent mixing with the main stream is sufficient to re-energise the separated flow, causing it to return to the surface and re-form a (turbulent) boundary layer. Clearly, the proximity of the reattachment point to the separation point will depend on how quickly transition sets in; in turn, this will depend on the stability of the laminar flow immediately downstream of the separation point, which can be described by the boundary layer velocity profile there. Now, the velocity distribution over the upper surface of a thin wing at incidence, near its leading edge, can be represented roughly by two straight lines; as the slopes of the lines and the maximum velocity are varied, the boundary layer thickness at the separation point alters, but the velocity profiles at separation remain similar.\*\* We may therefore describe the shape and scale of the boundary layer at the separation point by a single parameter defined by

$$(R\delta^*)_s = U_s \delta_s^* / \nu$$

where  $U_s$  is the main stream velocity outside the boundary layer and  $\delta_s^*$  is the displacement thickness, both measured at separation. Accordingly, the initial stability of the separated flow will be a function of  $(R\delta^*)_s$ .

From our knowledge of the behaviour of laminar wakes, to which the separated flow bears a certain resemblance, we can postulate a critical Reynolds number above which the flow is unstable. When instability sets in - it will be of the dynamic type and therefore comparatively violent - transition to turbulence occurs near to the separation point; "near" in this sense can be taken to mean within a few hundred displacement thicknesses. On the other hand, when  $(R\delta^*)_s$  is less than the critical value, the separated flow at first remains laminar for some distance downstream of the separation point and then, as the shape of its velocity profile changes, instability develops, eventually leading to turbulence. In this case the distance between the separation and transition points may be several thousand displacement thicknesses.

Of course, the condition for transition to turbulence is not sufficient to determine exactly where the flow becomes reattached to the

\* Especially in ref. 8 where hot-wire explorations of the region of separated flow are described.

\*\* This is most easily demonstrated by Howarth's method<sup>3</sup> of calculating a boundary layer flow subjected to a constant adverse velocity gradient.

surface or, indeed, whether reattachment occurs at all: we simply postulate transition as a necessary condition.\* For example, if the aerofoil incidence is large enough, separation persists in spite of transition. Clearly therefore, the geometry of the aerofoil must be taken into account if a precise description of the reattachment phenomenon is to be obtained.\*\* However, if we approach the problem less delicately, supposing that reattachment has occurred, and merely attempt to distinguish between the conditions for long and short bubbles, the elementary criterion based on  $(R\delta^*)_s$  should be adequate. On this basis, the following hypothesis is put forward: the bubble of separated flow will be long or short according to whether  $(R\delta^*)_s$  is less than or greater than a certain critical value.

#### 4 Analysis of experimental data

When a laminar boundary layer separates from the leading edge of an aerofoil, its thickness is small and, in general,  $(R\delta^*)_s$  cannot be deduced with sufficient accuracy from measurements of the boundary layer velocity profile; for this reason it is preferable to calculate  $(R\delta^*)_s$ . Two methods were used to calculate the growth of the laminar boundary layer, given the measured chordwise velocity distribution in the main stream; the first was to apply the Pohlhausen method<sup>3</sup> in the region of increasing velocity, joining on to Howarth's method<sup>2</sup> in the subsequent region of decreasing velocity: the second, and simpler, method was that given by Thwaites<sup>4</sup>. The two methods gave very nearly the same values of momentum thickness, displacement thickness and skin friction in the ranges of both favourable and unfavourable velocity gradient, as well as the location of the point of separation. Since Thwaites' method is the easier, it was used to calculate  $(R\delta^*)_s$  for other aerofoils. A comparison between the observed and estimated positions of the laminar separation point in a few typical cases is made in Table III.

TABLE III

Comparison between the observed and estimated positions of the laminar separation point

Incidence	$x_s/c$		
	Observed	Calculated	
		Thwaites	Pohlhausen-Howarth
<u>NACA 63-009 section</u>			
4°	0.021	0.025	0.021
6°	0.0215	0.022	0.022
8°	0.025	0.024	-
<u>NACA 63-012 section</u>			
10.8°	0.041	0.041	-

$x_s$  is the distance of the separation point from the front stagnation point, measured parallel to the aerofoil surface:  $c$  is the chord.

\* But only for the particular problem under discussion; at high subsonic or supersonic speeds for example, the mechanism of reattachment is different and the flow may remain laminar.

\*\* It is evident that the slope and curvature of the aerofoil profile at the separation point are important in this respect.

Observations of regions of laminar separation are not confined to thin aerofoils; data are also available on the laminar separation that occurs downstream of the minimum pressure point on moderately thick aerofoils,<sup>8,11</sup> again followed by turbulent reattachment.\* Other interesting data are provided by Gadd and Holder's observations at a Mach number of 2.0 of the interaction between an oblique shock wave and a laminar boundary layer on a flat plate<sup>5</sup>. It was found that at certain Reynolds number separation occurred upstream of the incident shock, followed by transition and reattachment. The region in which transition took place appeared to coincide with a kink in the pressure distribution along the surface of the plate and could therefore be approximately defined by the pressure measurements. In this way, the authors were able to deduce the distance between the points of separation and transition (roughly equal to the length  $\ell$  used here); they concluded that this distance was a function of the Reynolds number and did not depend on shock strength. Further experiments<sup>5</sup> showed that it was not greatly affected by change in Mach number; in fact, an increase in Mach number from 1.5 to 4.0 only altered  $\ell/\delta_s^*$  by a factor of 2. It will be shown later that the values of  $\ell/\delta_s^*$  deduced from these experiments are of the same order of magnitude as those obtained from experiments on aerofoils at low speeds within the same range of  $(R\delta^*)_S$ .

#### 4.1 Variation in the length of bubble with Reynolds number at separation

Values of  $\ell/\delta_s^*$  with corresponding values of  $(R\delta^*)_S$  are presented in Table VI, at the end of the paper, for a number of aerofoils<sup>1,2,7,8,10,11</sup> and for the shock wave experiments of Gadd and Holder<sup>5,6</sup>. To distinguish between experimental and calculated quantities:  $\ell$  is the length of bubble deduced from the experimental observations,  $\delta_s^*$  is the calculated displacement thickness at separation (for which the measured distribution of velocity outside the boundary layer is used), and in the Reynolds number  $(R\delta^*)_S$ , equal to  $U_S\delta_s^*/\nu$ ,  $U_S$  is the observed velocity just outside the boundary layer at the separation point.

Using the tabulated results,  $\log_{10} \ell/\delta_s^*$  is plotted against  $(R\delta^*)_S$  in Fig.2. The points in this figure fall strikingly into two distinct groups; one group for  $(R\delta^*)_S$  greater than 850, containing Gadd and Holder's supersonic measurements, clusters about the line  $\log_{10} \ell/\delta_s^* = 2$ , although there is a tendency for  $\ell/\delta_s^*$  to fall slightly with increasing Reynolds number. The other group,  $(R\delta^*)_S$  less than 500, lies between  $\log_{10} \ell/\delta_s^* = 3$  and  $\log_{10} \ell/\delta_s^* = 5$ . This behaviour is consistent with the hypothesis advanced in Section 3, and suggests that a critical Reynolds number, or band of Reynolds numbers, exists in the region 400-800, above which  $\ell/\delta_s^*$  is of order  $10^2$  - short bubbles - and below which  $\ell/\delta_s^*$  is more sensitive to changes in Reynolds number and may attain values of order  $10^4$  - long bubbles. The abruptness of the change in bubble length as the Reynolds number passes through the critical region can be better appreciated from Fig.3 where  $U_S\ell/\nu$  is plotted against  $(R\delta^*)_S$ .

Some further experimental evidence of a critical Reynolds number was brought to our attention by Sir Melvill Jones. He set his undergraduate students at Cambridge University a laboratory example which consisted of observing the change in the character of the flow about a thick aerofoil at zero incidence with change in Reynolds number or tunnel windspeed. At low Reynolds numbers a complete laminar separation occurred from the rear part of the aerofoil surface, then, as the Reynolds number was increased, transition appeared in the separated wake; at a sufficiently high Reynolds

\* For such aerofoils, the reattached boundary layer is not invariably turbulent, but for the purpose of the present analysis we shall only refer to experiments in which transition was known to occur in the separated flow.

number, the flow became reattached as a turbulent boundary layer. The gradual approach of the transition point in the separated layer to the separation point is analogous to the change from a long bubble to a short bubble in the case when separation is only transient. The Reynolds number at which separation was suppressed in the Cambridge experiment may therefore be compared with the critical Reynolds number suggested by Figs. 2 and 3. On analysis<sup>\*</sup>, it was found that the critical value of  $(R_{\delta^*})_s$  was 350, which is certainly of the same order of magnitude as that inferred from Figs. 2 and 3.<sup>\*\*</sup>

Clearly, more data are required to make the conclusions drawn from Figs. 2 and 3 really convincing: in particular, further observations on aerofoils with long bubbles are needed - the few points for Reynolds numbers less than 500 relate only to the N.A.C.A. 64-006 section and, with doubtful accuracy, to a double wedge section.<sup>\*\*\*</sup> On the other hand, further weight can be given to the conclusions by some more results on the N.A.C.A. 64-006 aerofoil. In Figs. 2 and 3 only points relating to long bubbles are shown, but it will be recalled from the description given in Section 2 that short bubbles were detected on this aerofoil at incidences less than  $5^\circ$ , the change from one type of bubble to the other occurring very suddenly. Calculations made for incidences of  $3^\circ$ ,  $4^\circ$  and  $4\frac{1}{2}^\circ$  led to values of  $(R_{\delta^*})_s$  which are compared in Table IV with corresponding values at higher incidences.<sup>\*\*\*\*</sup>

TABLE IV  
Relation between type of bubble and boundary layer  
Reynolds number at separation

Incidence degrees	$(R_{\delta^*})_s$	Type of bubble
3	480	short
4	480	short
$4\frac{1}{2}$	590	short
5	400	long
$5\frac{1}{2}$	310	long
6	390	long
7	410	long
8	380	long
9	390	long

- \* The authors are indebted to Mr. E.C. Maskell for the experimental observations recorded in his laboratory note-book.
- \*\* It may be noted that the wind tunnel in which the experiments were made had a high turbulence intensity, and so might be expected to encourage an early transition; this could explain why  $(R_{\delta^*})_{s,crit.}$  deduced from the Cambridge experiment is slightly lower than the band of values in Figs. 2 and 3. However, differences of this order are not significant since we cannot hope to define more than a rough magnitude of  $(R_{\delta^*})_{s,crit.}$
- \*\*\* It was necessary to guess part of the velocity distribution near the leading edge of the double-wedge section in order to calculate  $(R_{\delta^*})_s$ .
- \*\*\*\* It is clear from the pressure distributions given in ref. 2 that short bubbles were present at incidences less than  $5^\circ$  although no measurements of the lengths of these short bubbles were reported.

The  
bubb  
help  
whic  
tule

5

sepa  
bour  
valu  
rela  
gene  
crit  
turn  
the  
aero  
( $R_{\delta^*}$   
and  
prop  
line  
dist

exte

64-C

Anot  
also  
take  
hear

\* Th  
by  
vo  
fr  
me

re  
e  
short  
umber  
ere-  
2 and  
s 350,  
om

om  
on  
with  
n the  
ng  
in  
nces  
ng  
d to

l  
re  
o en-  
t.  
band  
re not  
mitudo

the  
( $R_{\delta^*}$ )<sub>s</sub>.  
short  
ure-

The results shown in Table IV indicate clearly a change from a short bubble to a long bubble as  $(R_{\delta^*})_s$  falls below 400. This observation helps to narrow the band of critical Reynolds number to roughly 400-500, which is of the order of magnitude found by Linke for transition to turbulence in the layer of separated flow behind a circular cylinder<sup>9</sup>.

5 Discussion

The criterion emerging from the analysis of Section 4 is that the separation bubble will be short if  $(R_{\delta^*})_s$  exceeds a value in the neighbourhood of 400-500 and will be long if  $(R_{\delta^*})_s$  lies below this band of values. It would, of course, be desirable to construct a rule which was related more obviously to the properties of the aerofoil section, but in general it is not possible to do this accurately since  $(R_{\delta^*})_s$  depends critically on the velocity distribution near the leading edge, which in turn is affected by the bubble. As a very rough approximation, however, the velocity distribution over the front part of the upper surface of the aerofoil may be represented by two straight lines. It then turns out that  $(R_{\delta^*})_s$  is proportional to  $(U_m x_m / \nu)^{1/2}$ , where  $U_m$  is the peak velocity and  $x_m$  its distance from the front stagnation point. The factor of proportionality is a function only of the ratio of the slopes of the two lines and may be treated as nearly constant for the class of velocity distributions typical of thin aerofoils at incidence.\* This is to some

extent borne out by the values of  $(R_{\delta^*})_s / \left( \frac{U_m x_m}{\nu} \right)^{1/2}$  for the N.A.C.A

64-006 and 63-009 aerofoil sections shown in Table V.

TABLE V

$$(R_{\delta^*})_s / \left( \frac{U_m x_m}{\nu} \right)^{1/2}$$

Aerofoil	Incidence degrees	$(R_{\delta^*})_s / \left( \frac{U_m x_m}{\nu} \right)^{1/2}$
NACA 64A006	5	3.2
	5 $\frac{1}{2}$	2.9
	6	3.6
	7	3.8
	8	3.4
NACA 63-009	9	4.2
	4	4.1
	6	3.5
	7	3.5
	8 $\frac{1}{2}$	3.8

Another interesting result of the two-line approximation is that  $U_s/U_m$  also is a function only of the ratio of the slopes and again might be taken as roughly constant for thin aerofoils; that this is, in fact, very nearly so can be seen from Fig.4 where the experimental values of  $U_s$  and

\* The conclusion that  $(R_{\delta^*})_s$  is proportional to  $(x_m)^{1/2}$  was also reached by Karman and Millikan<sup>15</sup> who used the two-line approximation to the velocity distribution. Their results are a little different numerically from those obtained in the present analysis by the Thwaites-Howarth method of calculating the laminar boundary layer.

$U_m$  are plotted. The ratio  $U_s/U_m$  from Fig.4 is 0.95; a similar analysis in ref.1 gave  $U_s/U_m = 0.94$ .

The relation between  $(R\delta^*)_s$  and  $(U_m x_m / \nu)^{1/2}$ , although of trivial theoretical interest, gives a useful clue to the connection between bubble length and type of aerofoil, since it is found from experiment that once a bubble forms the variation in  $U_m/U_0$  from one aerofoil to another (or, on a given aerofoil, from one incidence to another) is smaller than the variation in  $x_m/c$ . Accordingly, at a given Reynolds number (based now on aerofoil chord), long bubbles are associated with a forward position of the suction peak, which corresponds to small nose radius of curvature and thickness/chord ratio, or high incidence. This observation is supported by the analysis of  $C_{Lmax}$  in terms of nose radius of curvature (or, what is almost the same, the ratio of thickness at 0.05 chord to the chord,  $\tau_{0.05}$ ) made by Multhopp<sup>12</sup> who constructed curves of the measured  $C_{Lmax}$  for a number of aerofoils against  $\tau_{0.05}$ . These curves, in most instances, consisted of a flat portion for small values of  $\tau_{0.05}$  (see Fig.5, copied from ref.12) followed by a steep increase in  $C_{Lmax}$  with  $\tau_{0.05}$ , a flat maximum, and ultimately a gradual fall in  $C_{Lmax}$ . The change from the initially flat part of the curve to the rising part was abrupt and can be interpreted according to our present argument as a change from a long bubble to a short bubble on the aerofoil surface at incidences near to that of the stall.\*

The simple association between length of bubble and position of the suction peak can also be used to explain the stalling behaviour of certain sweptback wings. For instance, it is sometimes found from wind tunnel tests on thin wings at Reynolds numbers of the order of  $10^6$  that laminar separation occurs from the leading edge followed by reattachment, just as with two-dimensional aerofoils: but, in contrast to the two-dimensional case, the type of separation bubble is not constant across the span. Over the inboard parts of the leading edge the bubble is short, whereas over the outboard parts it is long; a trailing vortex sheet, called by Kuchemann<sup>13</sup> a part-span vortex sheet, separates the two flow regimes. If we consider only the flow component normal to the leading edge, the change in the type of bubble can be explained by means of the spanwise variation in the flow near the leading edge: because, at a given incidence, the increase in effective negative camber as the wing tip is approached leads to a progressive forward movement of the peak suction on the upper surface (the magnitude of the peak suction also increases, but its effect is outweighed by the forward movement). Consequently, conditions over the inboard parts of the wing favour a short bubble, while those outboard favour a long bubble. Apart from the complex stalling behaviour in circumstances like these, the presence of the trailing vortex sheet may influence the performance of a tailplane and a detailed knowledge of the flow pattern is therefore of great interest to the aeroplane designer. If the criterion suggested in this paper is correct, experiments made in a wind tunnel at a Reynolds number considerably below that descriptive of full-scale may not give reliable information about the effect of the part-span vortex sheet on the tailplane, since the position on the span where the bubble changes from short to long must depend on Reynolds number in such a way that it shifts outboard as the Reynolds number increases. This kind of qualitative conclusion is perhaps the most important to be drawn from the present analysis.

On two-dimensional aerofoils, the existence of a critical value for  $(R\delta^*)_s$  suggests a sudden change in stalling behaviour as the Reynolds

\* The rest of the curve - the flat maximum and gradual fall - can be explained in terms of a turbulent boundary layer separation starting near the trailing edge.

numl  
a Re  
gre:  
was  
ve:  
by:  
In f  
up i  
size  
to t  
stal

sect  
about  
bubb  
wise

6

for .  
Clea  
hypo  
obse  
is a  
made

meas  
seric  
on a  
flight  
parts  
distu  
separ  
proje

satis  
to ac  
lamin  
long  
encou  
stage  
point  
press  
cause  
pessi  
(or s  
thin

7.

lamin  
moder  
numbe  
bubbl  
or le

number increases. For example, tests on the N.A.C.A. 64-006 aerofoil at a Reynolds number of  $6 \times 10^6$  showed that a long bubble formed at incidences greater than  $5^\circ$ . According to our calculations, at  $9^\circ$  incidence  $(R\delta^*)_s$  was 390. Taking the critical value of  $(R\delta^*)_s$  to be between 400 and 500 we should predict that, at  $9^\circ$  incidence, the long bubble would be replaced by a short bubble at Reynolds numbers of from roughly  $7 \times 10^6$  to  $10 \times 10^6$ . In fact, the lift curves obtained from wind tunnel tests on this aerofoil up to a Reynolds number of  $9 \times 10^6$  gave no indication of a change in the size of bubble, although tests on the N.A.C.A. 0006 aerofoil<sup>14</sup>, which ought to behave similarly, showed a marked difference in the character of the stall between Reynolds numbers of  $6 \times 10^6$  and  $9 \times 10^6$ .

Extending the above argument to the sweptback wing with thin tip sections, it is clear that wind tunnel tests may give misleading information about the nature of the stall, especially the vicious tip stall, if a long bubble forming over the outboard portions of the model is reduced in spanwise extent or replaced by a short bubble at flight Reynolds numbers.

## 6 Future developments

The discussion given in this paper serves as a possible starting point for a more detailed investigation of the transient separation phenomenon. Clearly, a desirable first step is to check the validity of the elementary hypothesis relating the type of bubble to  $(R\delta^*)_s$ ; this can be done by observing the change in bubble length on an aerofoil as the Reynolds number is altered, and by a suitable choice of section the experiment could be made in a wind tunnel of moderate size.

If the hypothesis is substantiated, the extrapolation of wind tunnel measurements on sweptback wings to full-scale Reynolds numbers becomes a serious matter, as outlined in the previous Section. To obtain conditions on a model scale which might be comparable (qualitatively) with those in flight, a technique is needed to control the size of bubble on the outboard parts of the wing. One way of doing this in the tunnel is to introduce disturbances at the leading edge which precipitate transition in the separated layer; isolated roughness, perhaps in the form of small needles projecting from the surface, should suffice.

The ultimate problem, however, is one of design; the wing must have satisfactory stability and stalling characteristics and these are difficult to achieve without some sacrifice in the maximum usable lift coefficient if laminar separation bubbles are present, irrespective of whether they are long or short. It might be argued that the method suggested above for encouraging an early transition in the separated layer could be taken a stage further and used to induce transition ahead of the laminar separation point, but even this might not always be successful because the adverse pressure gradients near the tip of a sweptback wing can be sufficient to cause even a turbulent boundary layer to separate. These, possibly pessimistic, arguments point to the application of boundary layer suction (or some other kind of boundary layer control) to the leading edge of a thin sweptback wing, thereby eliminating the front separation altogether.

## 7 Conclusions

An elementary argument is put forward to relate the length of the laminar separation bubble that forms near the leading edge of a thin, or moderately thin, aerofoil at incidence, to the boundary layer Reynolds number,  $(R\delta^*)_s$  at the separation point. According to this argument, the bubble will be "short" or "long" depending on whether  $(R\delta^*)_s$  is greater or less than a certain critical value, corresponding to whether the flow

in the separated layer is initially unstable or stable to small disturbances. Available experimental data, obtained from low speed wind tunnel experiments on aerofoils and from some work at supersonic speeds on shock wave - boundary layer interaction, appear to support the hypothesis and suggest that the critical value of  $(R\delta^*)_s$  is in the region 400-500.

It follows that the length of bubble will be subjected to a scale effect. For example, a wing exhibiting a long bubble at a wind tunnel Reynolds number may have a short bubble at flight scale.

Although the analysis is confined to two-dimensional aerofoils, the results may be applied qualitatively to thin sweptback wings, in which case it becomes possible to explain the difference in the character of the stall between inboard and outboard portions of certain wings. Again, pronounced scale effects may be expected.

TABLE VI

Length of bubble and boundary layer Reynolds number at separation

Model		$e/\delta^*_s$	$(R\delta^*)_s$
Aerofoil, NACA 64A-006 Section	Incidence $5^\circ$	2144	401
	$5.5^\circ$	4990	312
	$6^\circ$	5440	393
	$7^\circ$	8800	406
	$8^\circ$	12890	378
	$9^\circ$	22580	389
Aerofoil, NACA 63-009 Section	Incidence $4^\circ$	63	1168
	$6^\circ$	77	869
	$7^\circ$	66	866
	$8^\circ$	46	910
Aerofoil, NACA 63-012 Section	Incidence $8.5^\circ$	46	976
	$10.8^\circ$	68	1209
Aerofoil, double-wedge Section	Incidence $6^\circ$	10300	494
Aerofoil, NACA 65, 3-018 Section	Incidence $0^\circ$	129	905
Aerofoil, NACA 66, 3-018 Section	Incidence $0^\circ$	90	1820
	$0.6^\circ$	87	2230
Aerofoil NACA 66, 2-516 Section	Incidence $3^\circ$	90	2510
Aerofoil NACA 66, 3-018 Section	Incidence $0^\circ$	76	2660
Aerofoil, 15: "roof-top" Section Shock wave-boundary layer expt.	Incidence $0^\circ$	25	4883
	$5^\circ$ wedge	96	1197
		92	1540
		84	1992
		76	2020
		61	2320
		66	2520
		38	3290
	$10^\circ$ wedge	144	1260
		141	1850
		112	2210
		81	2640
		76	3020
	$12^\circ$ wedge	246	960
	184	890	
	162	1260	
	156	1660	
	170	1740	
	114	2620	
	100	3100	

ir-  
nel  
rock  
id

the  
P  
in,

s

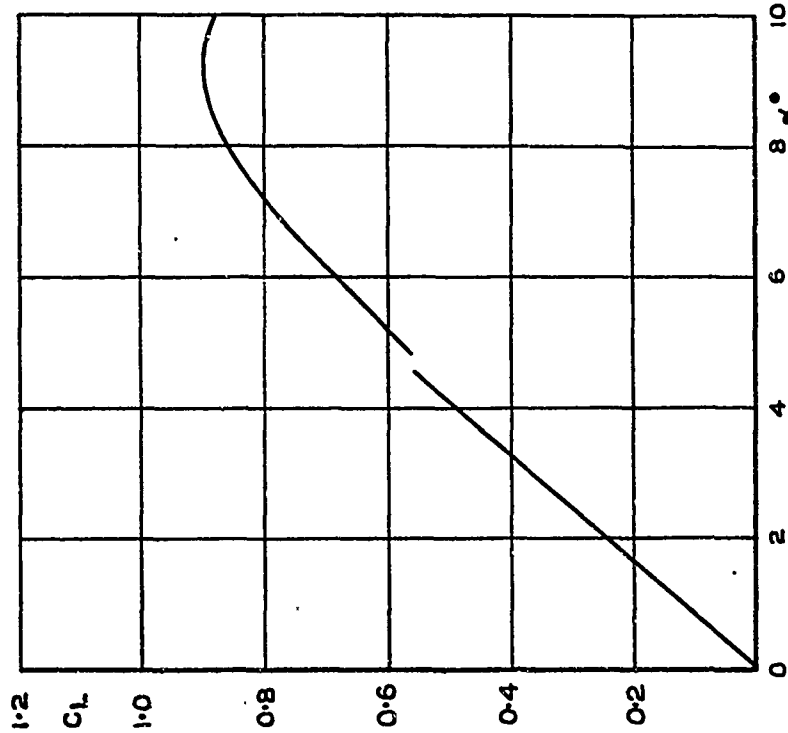
01  
12  
93  
06  
78  
89  
68  
69  
66  
10  
76  
09  
94  
05  
20  
30  
10  
60  
83  
97  
40  
92  
20  
20  
20  
90  
60  
50  
10  
40  
20  
60  
90  
60  
60  
40  
20  
00

REFERENCES

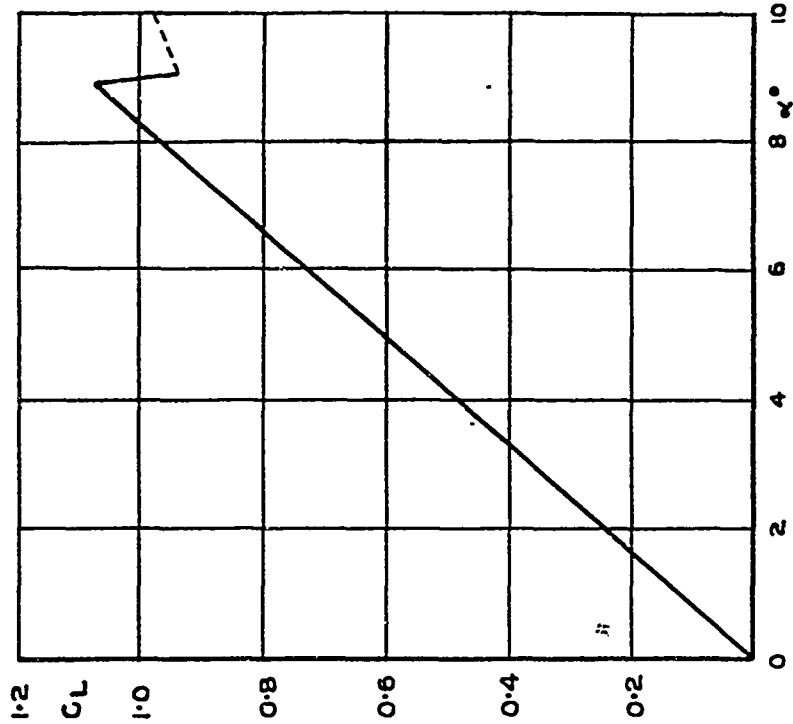
<u>No.</u>	<u>Author</u>	<u>Title, etc.</u>
1	D.E. Gault	Boundary layer and stalling characteristics of the N.A.C.A. 63-009 airfoil section N.A.C.A. Technical Note No. 1894 (1949)
2	G.B. McCullough and D.E. Gault	Boundary layer and stalling characteristics of the N.A.C.A. 64A006 airfoil section N.A.C.A. Technical Note No. 1923 (1949)
3	ed. S. Goldstein	Modern Developments in Fluid Dynamics Vol.I Chap.IV. Oxford (1938)
4	B. Thwaites	Approximate calculation of the laminar boundary layer Aeronautical Quarterly Vol.I (Nov.1949)
5	G.E. Gadd and D.W. Holder	The interaction of an oblique shock wave with the boundary layer on a flat plate Part I. A.R.C. 14848 (1952)
6	G.E. Gadd, D.W. Holder and J.D. Regan	The interaction of an oblique shock wave with the boundary layer on a flat plate Part II. A.R.C. 15591 (1953)
7	G.B. McCullough and D.E. Gault	An experimental investigation of the N.A.C.A.63,-012 Airfoil Section with leading edge suction slots N.A.C.A. Technical Note No. 1683 (1948)
8	W.J. Bursnall and L.K. Loftin	Experimental investigation of localised regions of laminar boundary layer separation N.A.C.A. Technical Note No. 2338 (1951)
9	ed.S. Goldstein	Modern Developments in Fluid Dynamics Vol.II Chap.XIII. Oxford (1938)
10	G.B. McCullough and D.E. Gault	Examples of three representative types of airfoil suction stall at low speed N.A.C.A. Technical Note No. 2502 (1951)
11	F. Cheers, W.S. Walker and C.R. Taylor	Two dimensional tests on a 15% thick symmetrical roof-top aerofoil with 20% plain flap in the NPL 13' x 9' wind tunnel R. & H. 2412. June, 1946
12	H. Multhopp	On the maximum lift coefficient of aerofoil sections R.A.E. Technical Note No. Aero 1980 (1948) A.R.C.12,115
13	D. Kuchemann	Types of flow on swept wings R.A.E. Technical Note No. Aero 2234 (1953)
14	I.H. Abbot, A.E. von Doenhoff and L.S. Stivers	Summary of airfoil data N.A.C.A. Report No. 824 (1945)

REFERENCES (Contd.)

<u>No.</u>	<u>Author</u>	<u>Title, etc.</u>
15	Th. von Kármán and C. B. Millikan	On the theory of laminar boundary layers involving separation. N.A.C.A. Report No. 504. (1954)



(a) NACA 64A006 SECTION



(b) NACA 63-009 SECTION

FIG. 1. LIFT CURVES FOR SECTIONS OF 6% AND 9% THICKNESS/CHORD RATIO 71  
6

(DATA TAKEN FROM REFS. 1 AND 2)

FIG. 2

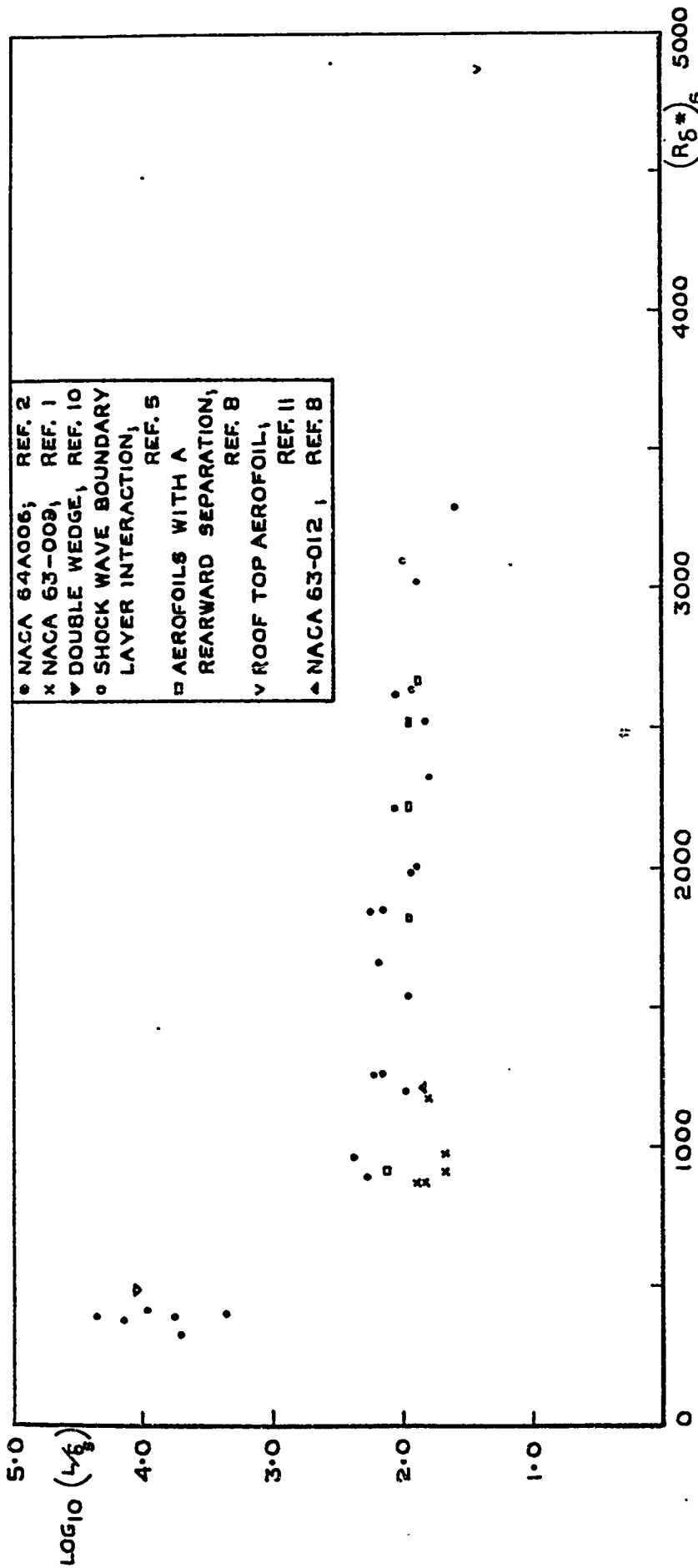


FIG. 2 VARIATION OF LENGTH OF SEPARATED FLOW REGION WITH BOUNDARY LAYER REYNOLDS N<sup>o</sup> AT THE SEPARATION POINT.

10-0

• NACA 64A006, REF. 2

11-8-10-6

FIG. 2 VARIATION OF LENGTH OF SEPARATION OF BOUNDARY LAYER REYNOLDS N<sub>0</sub> AT THE SEPARATION POINT.

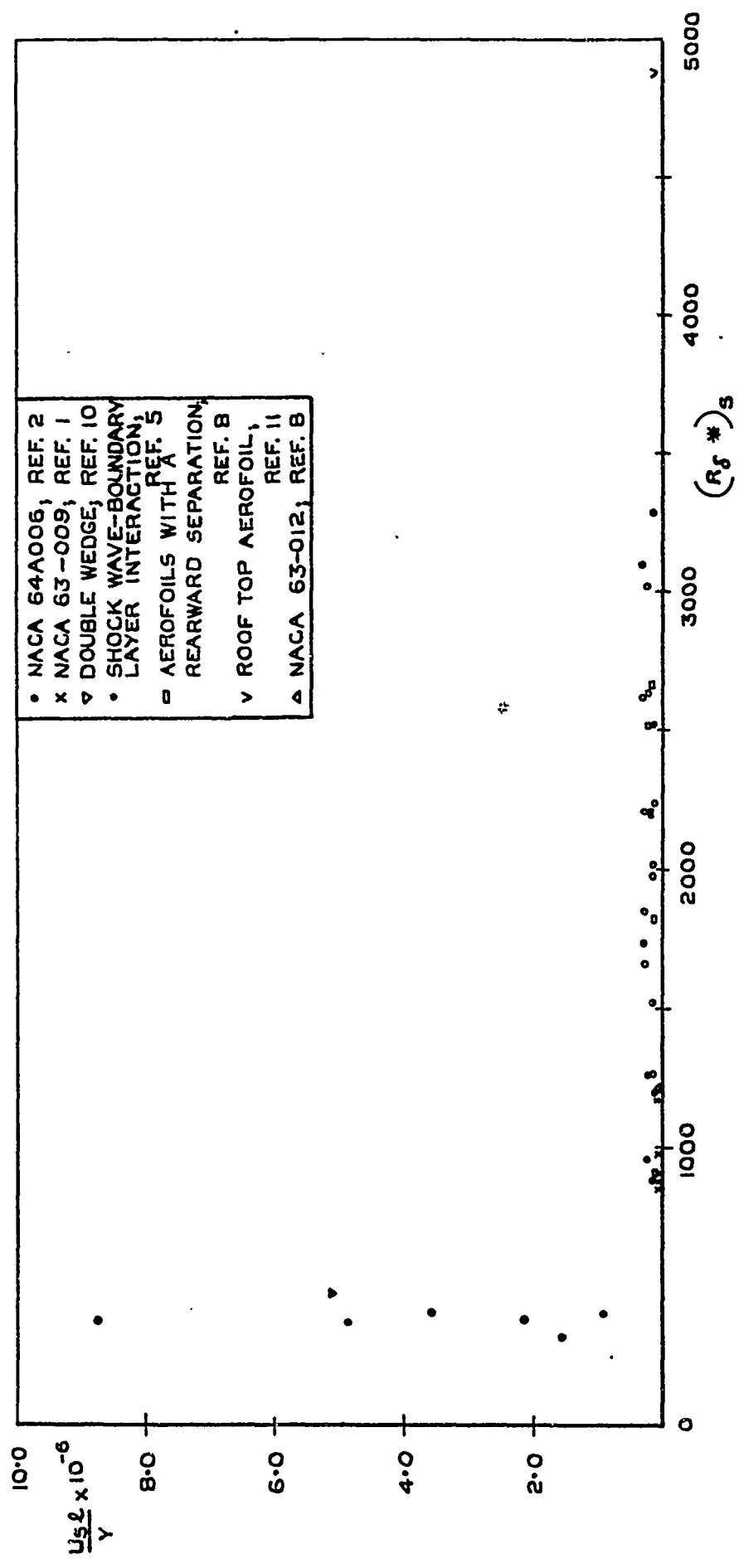


FIG. 3

FIG. 4

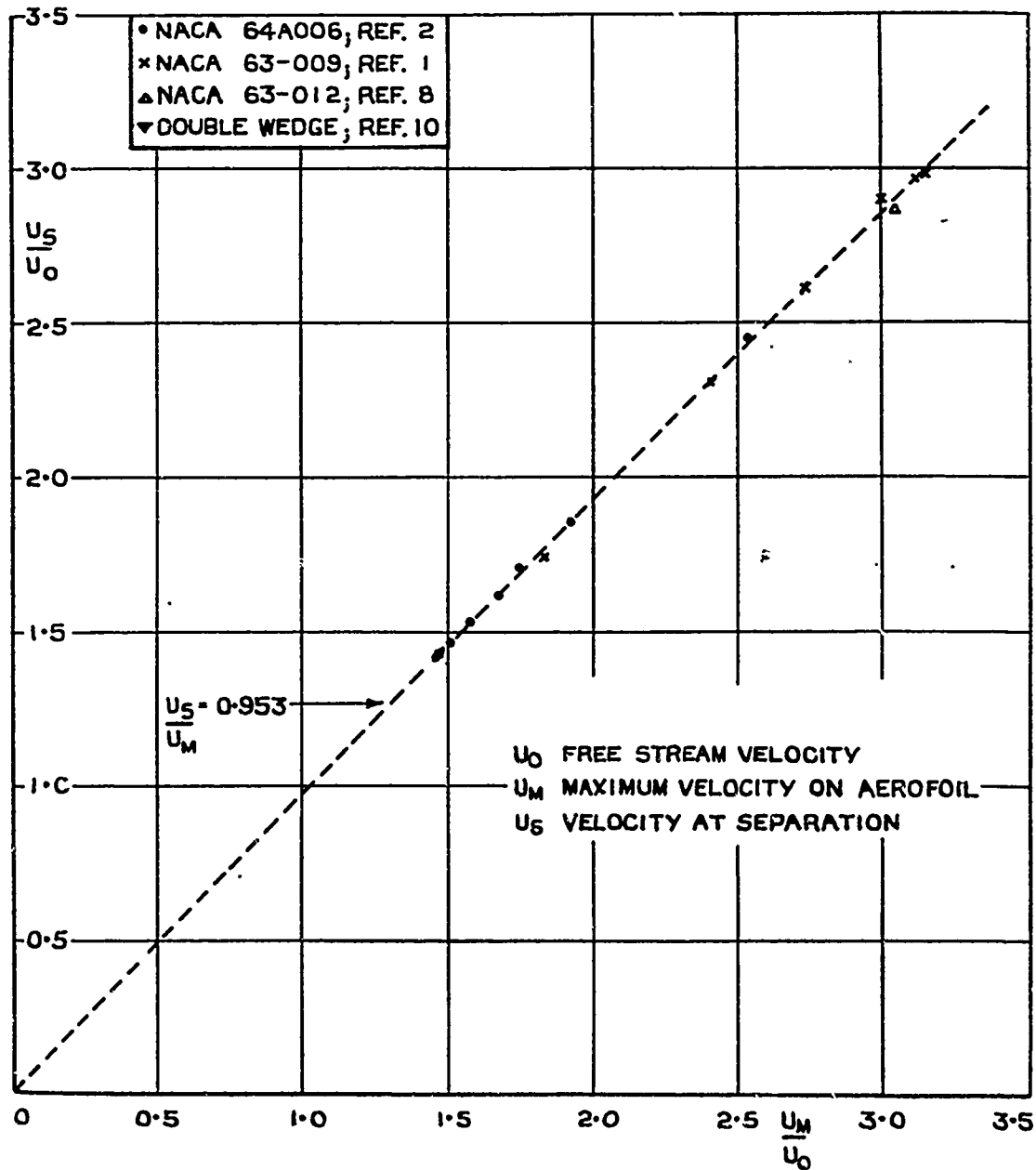


FIG. 4. RELATION BETWEEN VELOCITY AT SEPARATION AND MAXIMUM VELOCITY.

1.8

$C_{L\text{MAX}}$

FOIL

3-5

TY. AT

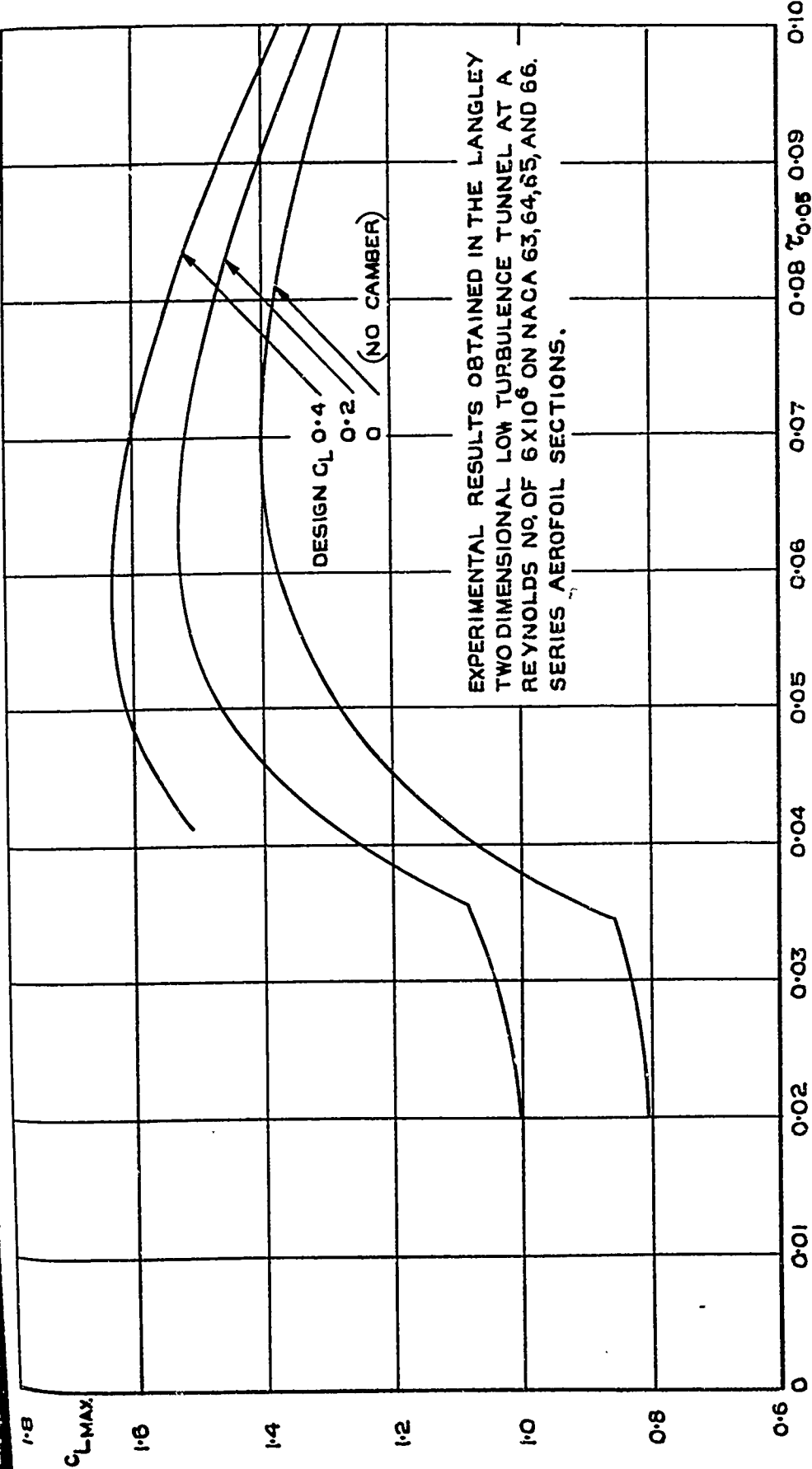


FIG. 5 MAXIMUM LIFT OF NACA CAMBERED AEROFOIL SECTIONS (ACCORDING TO MALTHOPP REF. 12.)

FIG. 5

dstl

dstl

Defense Technical Information Center (DTIC)  
8725 John J. Kingman Road, Suit 0944  
Fort Belvoir, VA 22060-6218  
U.S.A.

AD#: B952994  
Date of Search: 28 Sep 2009

Record Summary: AVIA 6/17974  
Title: Laminar Boundary Layer Separation from the Leading Edge of a Thin Aerofoil.  
Held by The National Archives, Kew

This document is now available at the National Archives, Kew, Surrey, United Kingdom.

DTIC has checked the National Archives Catalogue website (<http://www.nationalarchives.gov.uk>) and found the document is available and releasable to the public.

Access to UK public records is governed by statute, namely the Public Records Act, 1958, and the Public Records Act, 1967.

The document has been released under the 30 year rule.

(The vast majority of records selected for permanent preservation are made available to the public when they are 30 years old. This is commonly referred to as the 30 year rule and was established by the Public Records Act of 1967).

**This document may be treated as UNLIMITED.**